Angle-resolved photoemission from crystal-field split d shells of adsorbed atoms

J. W. Gadzuk
National Bureau of Standards, Washington, D.C. 20234
(Received 24 June 1975)

A theory of the angular distribution (AD) of photoemitted electrons from filled d shells of atoms adsorbed on solid surfaces is presented. The crystal field at the surface of the substrate splits the degenerate d states of the adsorbate into at least e_g and t_{2g} components. The angular distribution is then calculated for photoemission from the e_g group (since the distribution from the t_{2g} group is easily related to this). The final state is written as a partial-wave sum. For photoelectron kinetic energies less than about 10 eV, transitions from d to p partial waves dominate the AD and these AD's are azimuthally symmetric (for unpolarized light at normal incidence). Above 10 eV, the delayed onset (due to passing over the centrifugal barrier) of d to continuum f partial-wave emission occurs and this channel then dominates. The $d_{x^2-y^2}$ initial state, composed of spherical harmonics $Y_{2\pm2}$ is connected to $Y_{3\pm3}$ and $Y_{3\pm1}$ partial waves by the dipole operator. The calculated differential cross section, of the form $d\sigma/d\Omega = a(\theta) - b(\theta)\cos4\phi$, is fourfold symmetric, as expected, owing to interference effects between the $m = \pm1$ and $m = \pm3$ partial waves. The anisotropy parameter $\alpha(\theta) \equiv b(\theta)/a(\theta)$ changes sign at $\theta = 63.43°$ and this manifests itself as a 45° azimuthal rotation of the fourfold pattern. Specific systems for studying this effect experimentally are discussed. The deposition of Cu, Ag, or Au on a wide-band-gap insulator such as LiF appears promising as LiF should provide a large crystal field and the noble-metal d states should fall within the gap, thus remaining sharp and resolvable. The importance of the partial-wave interferences in other angle-resolved photoemission studies of oriented atoms, molecules, and surfaces is noted.

I. INTRODUCTION

Determinations of the differential photoionization cross section ($\equiv d\sigma/d\Omega$) for gas-phase atoms or molecules have been carried out for several years.[1,2] In the gas phase, the orientations of the atoms or molecules are random and thus the theoretical expressions for $d\sigma/d\Omega$ must be averaged over all possible orientations of the target. These random orientations preclude the possibility of gaining any structural information produced by the interference effects between electrons emitted from various centers in a molecule[3,4] and also necessitate some angular averaging of the interference effects between different partial wave channels in the final state. Consequently the differential cross section takes the form

$$\frac{d\sigma}{d\Omega} = \frac{\sigma(\epsilon)}{4\pi}\left[1 - \tfrac{1}{2}\beta(\epsilon)\,P_2(\cos\theta)\right], \tag{1}$$

where ϵ is the photoelectron energy, $\sigma(\epsilon)$ is the total photoionization cross section, $P_2(\cos\theta) = \frac{1}{2}(3\cos^2\theta - 1)$, θ is the angle between the photon and photoelectron directions (for unpolarized light), and $\beta(\epsilon)$ is the so-called asymmetry parameter which arises as follows. Using single-particle wave functions and LS coupling, it has been found[1,2] that $\beta(\epsilon)$ is

$$\beta(\epsilon) = \{l(l-1)R_{l-1}(\epsilon)^2 + (l+1)(l+2)R_{l+1}(\epsilon)^2 - 6l(l+1)R_{l-1}(\epsilon)R_{l+1}(\epsilon)\cos[\delta_{l+1}(\epsilon) - \delta_{l-1}(\epsilon)]\}/(2l+1)[lR_{l-1}(\epsilon)^2 + (l+1)R_{l+1}(\epsilon)^2], \tag{2}$$

where $R_{l\pm1}(\epsilon)$ are radial dipole matrix elements connecting the initial state of angular momentum l with the $l\pm1$ continuum partial waves and $\delta_{l\pm1}(\epsilon)$ are the phase shifts of these waves (with respect to free waves), due to electron-hole or excitonic interactions. Note that there is an interference term between the $l+1$ and $l-1$ outgoing channels which can change sign with energy as the difference in phase shifts of the two channels goes through odd integral multiples of $\frac{1}{2}\pi$. Due to the orientation averaging, there are no interference effects between waves with different m quantum numbers within a given l channel. In calculations of β, the radial matrix elements are determined from atomic initial-state functions and radial continuum functions which include the full effects of the hole potential. Finally, note that β always falls in the range $-1 \le \beta(\epsilon) \le +2$.

On the other hand, angle-resolved photoemission spectra (ARPS) of atoms adsorbed on solid surfaces have only recently been considered.[3-5] It has been shown that ARPS contain sufficient information to determine chemisorption bond geometry, i.e., positions of adatoms relative to substrate atoms, orbital shapes, and bond directions. The fundamental feature which distinguishes surface from gas-phase photoemission is the preferential orientation of the atoms or molecules due to the single-crystal surface. To date, two theories which highlight different aspects of ARPS from chemisorbed atoms and surface molecule complexes[6,7] have been presented.[3-5] In the theory by Gadzuk,[3-5] emphasis is placed on the anisotropies in an ARPS due to initial-state effects, as depicted in Fig. 1(a). In this diagram the adatom,

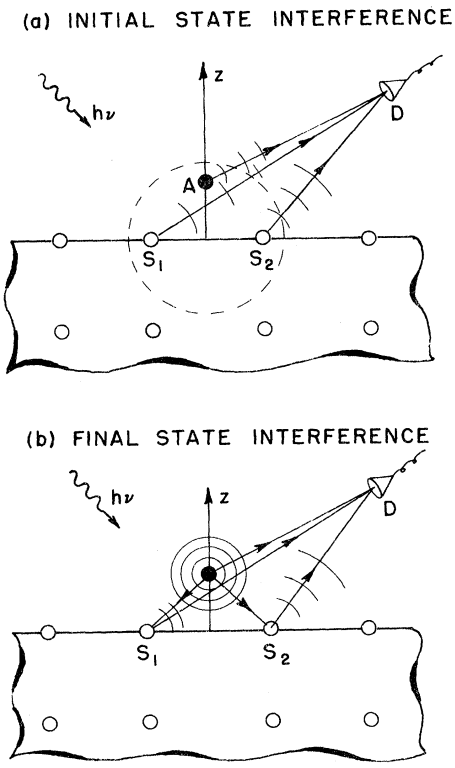

FIG. 1. Schematic surface molecule photoemission diagram which depicts the origins of interference effects. The adatom is labeled A, the nearest-neighbor substrate atoms S_1 and S_2, and the detector D. (a) In the initial state A, S_1, and S_2 act as coherent sources of electrons. (b) In the final state, electrons generated at A proceed directly to D, or propagate to S_1, S_2 where they are scattered back to the detector.

adsorbed in a bridge site, is assumed to form a chemical bond with the nearest-neighbor substrate d orbitals (for a transition metal) and the resulting photoionization is from such a molecular-orbital state. Thus, the amplitudes for photoionization from each of the three atomic centers in the surface molecule add with the result that interference effects are obtained because of the different path lengths AD, S_1D, and S_2D, and which depend on the geometrical structure of the molecule.[3,5] Since all adatoms adsorbed on a single-crystal face have the same orientations, these interference effects are not averaged out. In contrast, Liebsch[4,5] has stressed the anisotropies in the final-state wave function due to lattice backscattering of the photoelectrons from the adatom which are directed into the substrate, as shown in Fig. 1(b). In this case, the substrate atoms also act as sources with a definite relative phase compared to the adatom, due both to different path lengths and also the scattering phase shifts at S_1 or S_2 (although in reality, all substrate atoms ought to be included, the source strength decreases rapidly as the distance between the adatom and substrate atom increases). In both theories,[3,4] the simplifying approximation of taking the final state as a plane wave (modified by the lattice scattering) has been used, thus neglecting any final-state interactions between the excited electron and the localized hole. Within this approximation, it has been shown[5] that the differential photoionization cross section from an oriented, adsorbed atom possesses the form

$$\frac{d\sigma}{d\Omega} \sim \cos^2\gamma \left| \phi_a(\vec{p}) + \sum_j H_j(\vec{p}, \hat{\epsilon})\, e^{-i\vec{p}\cdot\vec{R}_j} \right|^2, \qquad (3)$$

where $\vec{p}$ is the wave vector of the photoelectron, γ is the angle between $\vec{p}$ and the photon polarization vector $\hat{\epsilon}$, $\phi_a(\vec{p})$ is the Fourier transform of the adatom valence orbital, $H_j(\vec{p}, \hat{\epsilon})$ is a complicated function depending on the parameters of the chemisorption bond[3] or the backscattering power,[4] $\vec{R}_j$ is the position of the jth substrate atom with respect to a coordinate system with its origin on the adatom, and the sum is over all substrate sites. If $|H_j| \approx |\phi_a|$ (within an order of magnitude) then interference effects result and a structural determination should be possible. Such a range seems likely in uv photoemission. A rather involved comparative discussion of these theories has been given in Ref. 5. Preliminary ARPS from adsorbate covered surfaces[8] and detailed ARPS from the layered material $TaSe_2$,[9] and the (111) face of Si,[10] indicate that the preferential (nonrandom) orientation of the atoms and chemical bonds at or near the surface of a solid do indeed lead to dramatic ARPS.

The purpose of the present paper is to present some new theoretical results on photoionization of atoms, within a solid state or surface environment. In particular, we consider the ARPS from a filled d shell of a layer of noninteracting adsorbed atoms on a single-crystal face of a cubic material. The wave function of the photoexcited electron is written as a partial-wave expansion and the various angular momentum components are solutions of a radial Schrödinger equation with a potential $V(r) + l(l+1)/r^2$, where $V(r)$ is the applicable atomic potential. By angular momentum selection rules, the d states can be excited only to continuum p and f partial waves, within the dipole approximation. Due to the centrifugal potential, the f waves have very small amplitudes in the region of the initial d state, near threshold energies, and thus the dominant photoexcitation is to continuum p waves. As the photoelectron energy is raised above the top of the centrifugal barrier (as much as 10–20 eV for Ag), a delayed onset[4] of photoionization into the f-wave channel occurs and this channel then dominates the photoionization process. Here we will consider how this effect appears in an ARPS from an oriented atom.

In Sec. II, general expressions for dipole matrix elements are calculated for an oriented atomic system. As an example, these results are then applied to the photoionization of Ag on a wide-band-gap insulator such as LiF in Sec. III. It is assumed that the strong crystal field of the ionic solid splits the degenerate d levels into at least e_g and t_{2g} groups which can be energy resolved. Since neither group is spherically symmetric, the ARPS from either group displays the symmetry of the crystal. As will be seen, these symmetries are due to interference effects between partial waves with different m quantum numbers, within a given l channel. This effect is washed out in gas-phase events due to the lack of a preferential direction for m quantization. Final discussion is given in Sec. IV.

II. DIPOLE MATRIX ELEMENTS

The differential photoionization cross section of the adsorbed atom is proportional to a modulus squared dipole matrix element[12]:

$$\frac{d\sigma}{d\Omega}=\kappa\,|\langle f|\hat{\epsilon}\cdot\vec{x}|i\rangle|^2\,, \tag{4}$$

where $\hat{\epsilon}$ is the photon polarization, $\vec{x}$ is the dipole operator, and κ is a group of constants depending on $h\nu$, the photon energy. Unlike the gas phase, special care must be exercised to express all quantities in the coordinate system set by the crystal axis. The initial atomic state for an orbital with quantum numbers n and l' is

$$|i\rangle=R_{nl'}(r)\sum_{m'}n(m')|l'm'\rangle, \tag{5}$$

where $R_{nl'}(r)$ is the radial wave function, $|l'm'\rangle$ is a spherical harmonic, and the $n(m')$'s are coefficients needed to form directed orbitals with cubic symmetry.[13] Following Cooper and Zare,[1] the final state, satisfying ingoing wave boundary conditions, is written as a partial-wave expression

$$|f\rangle=4\pi\sum_{lm}(i)^l e^{-i\delta_l}Y^*_{lm}(\hat{k})\,Y_{lm}(\hat{r})\,G_{\epsilon l}(r), \tag{6}$$

where δ_l is the lth wave phase shift due to the hole potential, $\hat{k}$ is the direction of the outgoing electron, $\hat{r}$ the angle associated with the spatial coordinate of the electron, and $G_{\epsilon l}(r)$ a continuum radial wave function which is a solution of the Schrödinger equation with the correct hole potential. Using Eqs. (5) and (6), the dipole matrix element is

$$\begin{aligned}\langle f|\hat{\epsilon}\cdot\vec{x}|i\rangle=\sum_{l,m,m'}n(m')\,a(l,m)\,R_l(\epsilon)\langle lm|\,\epsilon_x(x/r)\\+\epsilon_y(y/r)+\epsilon_z(z/r)|l'm'\rangle,\end{aligned} \tag{7}$$

with $\epsilon_{x,y,z}$ the respective components of the polarization vector,

$$a(l,m)\equiv 4\pi(i)^l e^{-i\delta_l}Y_{lm}(\hat{k}),$$

and $R_l(\epsilon)$ the radial matrix element

$$R_l(\epsilon)\equiv\int_0^\infty r R_{nl'}(r)\,G_{\epsilon l}(r)\,dr.$$

Writing the position operators in terms of Y_{lm}'s

$$x/r=(\tfrac{2}{3}\pi)^{1/2}(-Y_{11}+Y_{1-1}),$$
$$y/r=i(\tfrac{2}{3}\pi)^{1/2}(Y_{11}+Y_{1-1}),$$
$$z/r=(\tfrac{4}{3}\pi)^{1/2}Y_{10},$$

Eq. (7) becomes

$$\begin{aligned}\langle f|\hat{\epsilon}\cdot\vec{x}|i\rangle=\sum_{l,m,m'}n(m')\,a(l,m)\,R_l(\epsilon)\,(\tfrac{2}{3}\pi)^{1/2}\\\times[\epsilon_x(-\langle lm|\,Y_{11}\,|l'm'\rangle\\+\langle lm|\,Y_{1-1}\,|l'm'\rangle)+i\epsilon_y(\langle lm|\,Y_{11}\,|l'm'\rangle\\+\langle lm\,|\,Y_{1-1}\,|l'm'\rangle)+\sqrt{2}\,\epsilon_z\langle lm|\,Y_{10}\,|l'm'\rangle].\end{aligned} \tag{8}$$

The angular matrix elements whose integrands are products of three spherical harmonics are tabulated Gaunt coefficients[14] given by the expression[15]

$$\langle lm|\,k,m-m'\,|l'm'\rangle=[(2k+1)/4\pi]^{1/2}\,C^k(lm,l'm').$$

In fact all the nonvanishing matrix elements in Eq. (8) are of the form

$$\begin{aligned}\langle lm|\,11\,|l'm'\rangle&=(3/4\pi)^{1/2}\,C^1(l\,m'+1,\;l'\,m'),\\\langle lm\,|\,1-1\,|l'm'\rangle&=(3/4\pi)^{1/2}\,C^1(l\,m'-1,\;l'm'),\\\langle lm|\,10\,|l'm'\rangle&=(3/4\pi)^{1/2}C^1(l\,m',l'm'),\end{aligned} \tag{9}$$

which expresses the dipole angular momentum selection rule $\Delta l=\pm1$, $\Delta m=\pm1,0$. With the insertion of Eq. (9) into (8) and some rearrangement, a generalized form of the oriented dipole matrix element is obtained:

$$\begin{aligned}\langle f|\hat{\epsilon}\cdot\vec{x}|i\rangle=\sum_{lm'}n(m')\,\frac{R_l(\epsilon)}{\sqrt{2}}[(-\epsilon_x+i\epsilon_y)\,a(l,m'+1)\\\times C^1(l,m'+1;\;l'm')+(\epsilon_x+i\epsilon_y)\,a(l,m'-1)\\\times C^1(l,m'-1;\;l'm')\\+\sqrt{2}\,\epsilon_z\,a(l,m')\,C^1(l,m';\;l'm')].\end{aligned} \tag{10}$$

In dealing with either normal-incidence linearly polarized or unpolarized photons, Eq. (10) can be regrouped into the more convenient form

$$\begin{aligned}\langle f|\hat{\epsilon}\cdot\vec{x}|i\rangle=\sum_{lm'}n(m')\,\frac{R_l(\epsilon)}{\sqrt{2}}\\\times\{\epsilon_x[-a(l,m'+1)\,C^1(l,m'+1;\;l'm')\\+a(l,m'-1)\,C^1(l,m'-1;\;l'm')]\\+i\epsilon_y[a(l,m'+1)\,C^1(l,m'+1;\;l'm')\end{aligned}$$

$$+a(l, m'-1)\,C^1(l, m'-1;\ l'\ m')]$$
$$+\sqrt{2}\,\epsilon_z a(l, m')\,C^1(l, m';\ l'm')\},\qquad (11)$$

where it can be noted that for normal incidence $\epsilon_z = 0$ and thus all transitions satisfy the selection rule $\Delta m = \pm 1$. In the example to follow, we will consider only the experiment with unpolarized light at normal incidence. Then the ARPS are obtained by an incoherent sum of linear x and y polarized ARPS. To proceed beyond here, specific orbitals must be considered.

III. CRYSTAL-FIELD-SPLIT d SHELLS

As a specific example of the concepts presented in Sec. II, consider the case of Ag adsorbed on a wide-band-gap insulator such as LiF. We chose Ag since, in the gas phase, the centrifugal barrier is known to cause a delayed onset into the continuum f channel by ~20 eV.[11] Furthermore, since the ionization potential of the d electrons is ~12 eV in the gas phase and ~10 eV in the solid state, uv photoemission with the He resonance lines should be possible. LiF is suggested for two reasons. First, a strong crystal field is present to split the degenerate d shell. For octahedral fields, the upper e_g level is doubly degenerate ($d_{x^2-y^2}$, d_{z^2}) whereas the lower t_{2g} level is triply degenerate (d_{xy}, d_{yz}, d_{zx}). In a surface crystal field,[16,17] each of these groups should again be split (d_{yz} and d_{zx} remaining degenerate for a simple-cubic face) due to the reduction of symmetry in the z direction. Second, the possibility exists that these levels will have energies within the band gap and thus will remain sharp and easily resolvable. Due to the fact that the sum of the charge densities in the filled d shell (two e_g and three t_{2g} orbitals doubly occupied) is spherically symmetric, the total differential cross section for unpolarized light at normal incidence is isotropic in ϕ. Thus $d\sigma_{t_{2g}}/d\phi + d\sigma_{e_g}/d\phi = 0$ and calculating one of these is sufficient.

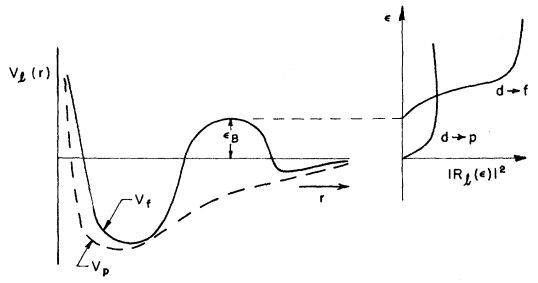

FIG. 2. Form of the final-state potentials seen by the p and partial waves on the left-side and squares of the partial wave radial matrix elements, as a function of energy, on the right-side. Note that the $d \rightarrow f$ matrix element is small for $\epsilon \lesssim \epsilon_B$, the centrifugal barrier.

TABLE I. Angular expressions for spherical-harmonic combinations.

Spherical harmonics		Trigonometric functions
$\mp Y_{1-1} + Y_{11}$	=	$-\left(\frac{3}{2\pi}\right)^{1/2} \sin\theta \times \begin{cases} i\sin\phi \\ \cos\phi \end{cases}$
$\mp Y_{33} + Y_{3-3}$	=	$\left(\frac{35}{16\pi}\right)^{1/2} \sin^3\theta \times \begin{cases} \cos 3\phi \\ -i\sin 3\phi \end{cases}$
$\mp Y_{3-1} + Y_{31}$	=	$-\left(\frac{21}{16\pi}\right)^{1/2} \sin\theta(5\cos^2\theta - 1) \times \begin{cases} \cos\phi \\ i\sin\phi \end{cases}$

Some additional features of the proposed experiment are illustrated in Fig. 2. Photoexcitation is possible either by $d \rightarrow f$ or $d \rightarrow p$ transitions. The effective potential seen by the p (f) wave is labeled V_p (V_f). Note the presence of the centifugal barrier in V_f which limits the $d \rightarrow f$ processes for $\epsilon \lesssim \epsilon_B$, the barrier height. As ϵ increases above ϵ_B, f waves have increased amplitudes near the atom and $d \rightarrow f$ excitations are then possible. This is the origin of the phrase "delayed onset." Schematic forms for the energy dependence of the squared radial matrix elements are shown on the right-hand side of Fig. 2. In general, above the delayed onset threshold, the strength in the $d \rightarrow f$ channel is much greater than that in the $d \rightarrow p$ channel.

A. $d \rightarrow p$ transitions

First we consider the transition from the $d_{x^2-y^2}$ orbital.[13] The factor $n(m' = \pm 2) = 1/\sqrt{2}$ and equals zero for all other m'. The Gaunt coefficient $C^1(1, m' \pm 1;\ 2,\ \pm 2) = -\sqrt{\frac{6}{15}}$. Consequently, from Eq. (11), the dipole matrix element is

$$\langle p|\hat{\epsilon}\cdot\vec{x}\,|\,x^2-y^2\rangle = R_p(\epsilon)\ 2\pi\sqrt{\tfrac{6}{15}}\,[\epsilon_x(-Y_{1-1}+Y_{11}) + i\epsilon_y(Y_{1-1}+Y_{11})]\ e^{-i(\delta_p-\pi/2)}.\qquad (12)$$

With the spherical harmonics in Eq. (12) expressed as the trigonometric functions shown in Table I, the modulus squared dipole matrix element for unpolarized light is

$$|\langle p|\hat{\epsilon}\cdot\vec{x}\,|\,x^2-y^2\rangle|^2_{\text{unpol}} = R_p^2(\epsilon)\tfrac{12}{15}\pi(|-Y_{1-1}+Y_{11}|^2 + |Y_{1-1}+Y_{11}|^2) = R_p^2(\epsilon)\tfrac{12}{5}\pi\sin^2\theta.\qquad (13)$$

In an octahedral field, d_{z^2} is degenerate with $d_{x^2-y^2}$, and so must also be included. (Although as mentioned earlier, this degeneracy may be split to a resolvable degree by the surface crystal field.) For this case, $n(m' = 0) = 1$, $C^1(1, \pm 1;\ 2, 0) = \sqrt{\frac{1}{15}}$, and Eq. (11) becomes

$$\langle p|\hat{\epsilon}\cdot\vec{x}\,|\,z^2\rangle = R_p(\epsilon)\sqrt{\tfrac{1}{30}}\,[\epsilon_x(-Y_{11}+Y_{1-1}) + i\epsilon_y(Y_{11}+Y_{1-1})]\ e^{-i(\delta_p-\pi/2)},$$

which yields

$$|\langle p|\hat{\epsilon}\cdot\vec{x}|z^2\rangle|^2_{\text{unpol}} = R_p^2(\epsilon)\tfrac{4}{5}\pi\sin^2\theta. \quad (14)$$

Combining Eqs. (13) and (14), the total differential cross section for $d \to p$ transitions is

$$\frac{d\sigma_{\text{tot}}(d\to p)}{d\Omega} = \kappa R_p^2(\epsilon)\tfrac{16}{5}\pi\sin^2\theta, \quad (15)$$

which is independent of the azimuthal angle ϕ and is not very interesting.

B. $d \to f$ transitions

The novel features in the ARPS arise when the photoelectron energy is above the delayed onset threshold for excitation into the f channel. For the case of the $d_{x^2-y^2}$ orbital, the dipole operator connects this orbital with both f, $m=\pm 3$ and f, $m=\pm 1$ partial waves. Interference effects between these waves lead to some intriguing consequences. Again $n(m')=1\sqrt{2}\,\delta_{m,\pm 2}$, but now the only nonvanishing Gaunt coefficients are $C^1(3,\mp 2\pm 1;\ 2,\mp 2)=\sqrt{\frac{15}{35}}$ and $C^1(3,\mp 2\mp 1;\ 2,\mp 2)=\sqrt{\frac{1}{35}}$. Thus Eq. (11) becomes

$$\begin{aligned}\langle f(l=3)|\hat{\epsilon}\cdot\vec{x}|x^2-y^2\rangle &= R_f(\epsilon)(2\pi/\sqrt{35})[\epsilon_x(-\sqrt{15}\,Y_{33}-Y_{3-1}+Y_{31}+\sqrt{15}\,Y_{3-3})\\ &+ i\epsilon_y(\sqrt{15}\,Y_{33}+Y_{3-1}+Y_{31}+\sqrt{15}\,Y_{3-3})]\,e^{-i(\delta_f+\pi/2)}.\end{aligned} \quad (16)$$

For the spherical harmonics shown in Table I, Eq. (16) is

$$\begin{aligned}\langle f(l=3)|\hat{\epsilon}\cdot\vec{x}|x^2-y^2\rangle &= R_f(\epsilon)\frac{2\pi}{\sqrt{35}}\Bigg\{\epsilon_x\Bigg[\left(\frac{15\times 35}{16\pi}\right)^{1/2}\sin^3\theta\cos 3\phi\\ &-\left(\frac{21}{16\pi}\right)^{1/2}\sin\theta(5\cos^2\theta-1)\cos\phi\Bigg]\\ &+\epsilon_y\left(\frac{15\times 35}{16\pi}\right)^{1/2}\sin^3\theta\sin 3\phi\\ &+\left(\frac{21}{16\pi}\right)^{1/2}\sin\theta(5\cos^2\theta-1)\sin\phi\Bigg\}e^{-i(\delta_f+\pi/2)}.\end{aligned} \quad (17)$$

Taking the modulus squared and manipulating some terms we see that Eq. (17) leads to

$$\begin{aligned}|\langle f(l=3)|\hat{\epsilon}\cdot\vec{x}|x^2-y^2\rangle|^2_{\text{unpol}} &= R_f^2(\epsilon)\pi[\tfrac{15}{4}\sin^6\theta+\tfrac{3}{20}\sin^2\theta(5\cos^2\theta-1)^2\\ &-\tfrac{3}{2}\sin^4\theta(5\cos^2\theta-1)\cos 4\phi],\end{aligned} \quad (18)$$

where use has been made of the identity $-\cos 3\phi\cos\phi+\sin 3\phi\sin\phi=-\cos 4\phi$. The term which depends on ϕ in Eq. (18) arises from interferences between the $Y_{3\pm 3}$ and $Y_{3\pm 1}$ channels and averages to zero in gas-phase theories.

In the case of the d_z^2 orbital, $n(m')=\delta_{m'0}$ and $C^1(3,\pm 1;\ 2,0)=\sqrt{\frac{6}{35}}$ so Eq. (11) yields

$$\begin{aligned}\langle f(l=3)|\hat{\epsilon}\cdot\vec{x}|z^2\rangle &= R_f(\epsilon)4\pi\sqrt{\tfrac{3}{35}}[\epsilon_x(-Y_{31}+Y_{3-1})\\ &+ i\epsilon_y(Y_{31}+Y_{3-1})]\,e^{-i(\delta_f+\pi/2)},\end{aligned}$$

which easily gives

$$\begin{aligned}|\langle f(l=3)|\hat{\epsilon}\cdot\vec{x}|z^2\rangle|^2_{\text{unpol}} &= R_f^2(\epsilon)\pi\tfrac{9}{5}\sin^2\theta(5\cos^2\theta-1)^2.\end{aligned} \quad (19)$$

Thus the total $d_{e_g}\to f$ differential cross section, from Eqs. (18) and (19), is

$$\begin{aligned}\frac{d\sigma_{\text{tot}}(d_{e_g}\to f)}{d\Omega} &= \kappa R_f^2(\epsilon)\tfrac{1}{4}\pi[15\sin^6\theta\\ &+\tfrac{39}{5}\sin^2\theta(5\cos^2\theta-1)^2\\ &-6\sin^4\theta(5\cos^2\theta-1)\cos 4\phi],\end{aligned} \quad (20)$$

which does display some interesting properties. Polar plots of $d\sigma_{\text{tot}}/d\Omega$ vs ϕ, treating θ parametrically are shown in Fig. 3. Although the absolute scale is arbitrary, the relative intensities between these curves are correct. As might be intuitively evident, the intensities display fourfold symmetry due to $d_{x^2-y^2}$. What is unexpected is that for larger θ, the position of the maximum intensity is rotated by 45°. The origin of this behavior is the interferences between the $Y_{3\pm 3}$ and $Y_{3\pm 1}$ partial waves. Since there are interference effects, the sign or relative phases between these channels gives rise to observable consequences. Since $Y_{3\pm 1}\sim\sin\theta(5\cos^2\theta-1)$ whereas $Y_{3\pm 3}\sim\sin^3\theta$, the interference terms of the form $Y_{3\pm 1}Y^*_{3\pm 3}\sim\sin^4\theta(5\cos^2\theta$

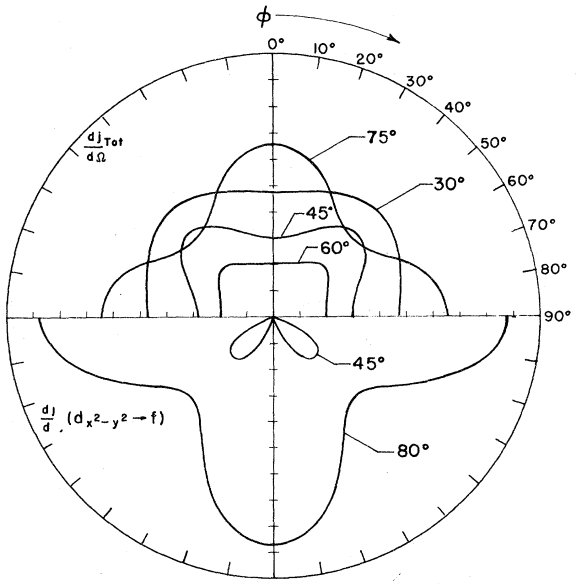

FIG. 3. Azimuthal ARPS for photoejection of crystal-field-split d-shell electrons, by normal incidence, unpolarized light. The polar angle θ is treated parametrically. In the upper half-plane, the ARPS are for emission from the e_g group whereas in the lower half-plane, the ARPS are for emission from only the $d_{x^2-y^2}$ orbital.

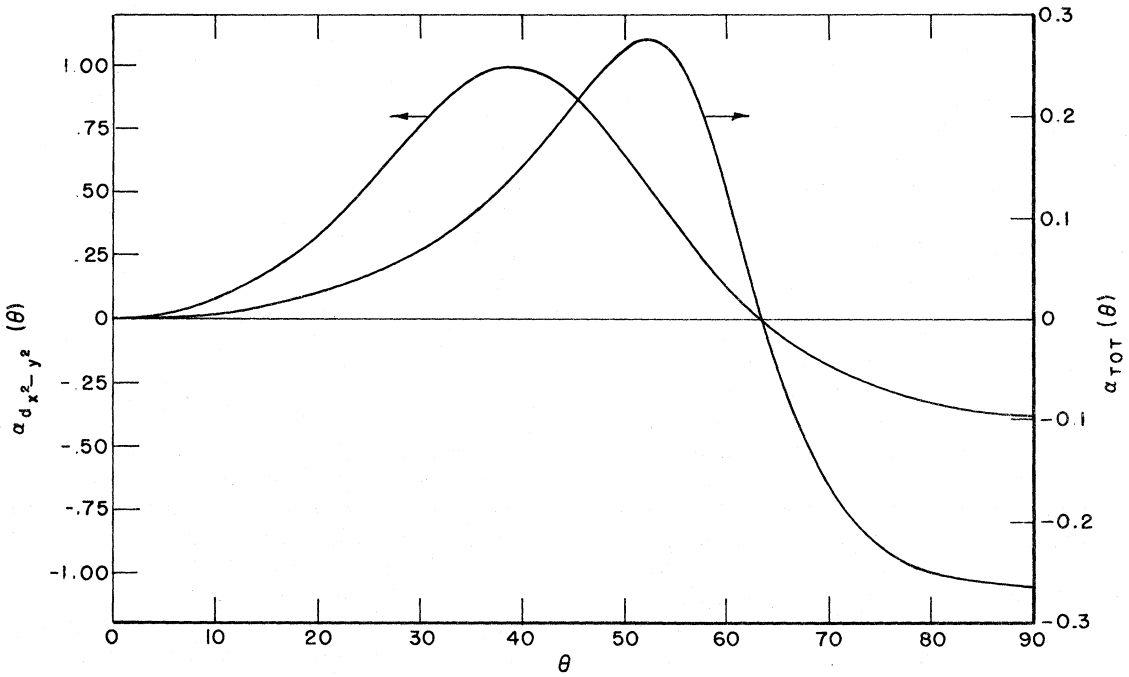

FIG. 4. The anisotropy parameter α as a function of polar angle. The right-hand scale refers to total e_g emission whereas the left-hand scale refers to $d_{x^2-y^2}$ emission only.

-1) change sign at $\theta=\cos^{-1}(1/\sqrt{5})=63.43°$ (where the ARPS is isotropic in ϕ) and it is this effect which accounts for the rotation of the ARPS maxima by $\phi=45°$.

It is convenient to define an anistropy parameter

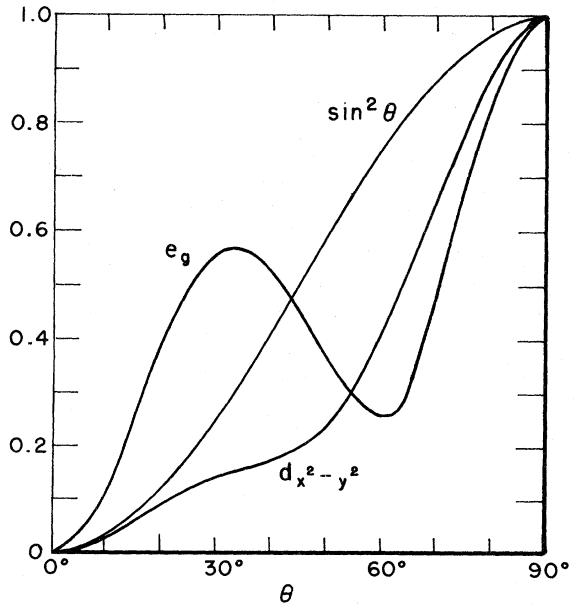

FIG. 5. Maximum intensity ($\phi=0$ or $\frac{1}{4}\pi$) as a function of polar angle for e_g and $d_{x^2-y^2}$ emission, compared to a simple $\sin^2\theta$ behavior.

$\alpha(\theta)$ as follows. From either Eq. (18) or (20) it can be noted that the structure of the differential cross section is

$$\frac{d\sigma}{d\Omega}=a(\theta)-b(\theta)\cos4\phi$$
$$=a(\theta)[1-\alpha(\theta)\cos4\phi], \tag{21}$$

with $\alpha(\theta)\equiv b(\theta)/a(\theta)$, and which is a measure of the azimuthal variation of the cross section relative to the ϕ independent part. The fractional variation is $2\alpha(\theta)$. The anisotropy parameter for total $d\rightarrow f$, and $d_{x^2-y^2}\rightarrow f$, transitions are given, respectively, by

$$\alpha_{tot}(\theta)=6\sin^2\theta(5\cos^2\theta-1)/[15\sin^4\theta$$
$$+\tfrac{39}{5}(5\cos^2\theta-1)^2]$$

and

$$\alpha_{x^2-y^2}(\theta)=6\sin^2\theta(5\cos^2\theta-1)/[15\sin^4\theta$$
$$+\tfrac{3}{5}(5\cos^2\theta-1)^2],$$

which are plotted in Fig. 4. Note that at the "magic angle" of $\theta=63.43°$, $\alpha=0$. Obviously the anisotropy of an observed ARPS will be enhanced if the surface crystal field does split the e_g group and one can look at the emission from the $d_{x^2-y^2}$ orbital by itself.

Finally note that in addition to an optimal θ [where $|\alpha(\theta)|$ is maximum] for maximum anisotropy, there are best polar angles for maximum intensity. From the plot of $d\sigma(\phi=0,\frac{1}{4}\pi)/d\Omega=a(\theta)+|b(\theta)|$ shown in Fig. 5, the departures from a

simple $\sin^2\theta$ dependence are seen.

IV. CONCLUSIONS

In summary, the points of the present paper are the following. An analysis of the differential photoionization cross section of an oriented atomic orbital has been given within the dipole formulation. It has been suggested that experiments performed on systems of adsorbed atoms (or implanted impurities[18]) on (or in) hosts which provide crystal fields might lead to some novel possibilities. In particular we have focused on the crystal-field splitting of a filled d shell into e_g and t_{2g} components and the resulting ARPS from one such component. Due to interference effects between different partial waves in a given l channel, anisotropies in the ARPS are predicted which should be related to the local geometry of the emitting atom, e.g., as felt in the crystal field. This new geometrical effect is completely different from the initial and final state anisotropies discussed previously by Gadzuk[3,5] and Liebsch.[4,5] The ultimate solution to the angle-resolved photoemission problem must include the influences of all three effects although any given experimental system may favor one over the others.[19]

---

[1] J. Cooper and R. N. Zare, J. Chem. Phys. 48, 942 (1968); and *Lectures in Theoretical Physics, Atomic Collision Processes*, (Gordon and Breach, New York, 1969), Vol. XI C.

[2] D. J. Kennedy and S. T. Manson, Phys. Rev. A 5, 227 (1972); T. A. Carlson, G. E. McGuire, A. E. Jonas, K. L. Cheng, C. P. Anderson, C. C. Lu, and B. P. Pullen, in *Electron Spectroscopy* edited by D. A. Shirley (North-Holland, Amsterdam, 1972); J. W. Rabalais and T. P. Debies, J. Elec. Spectrosc. 5, 847 (1974).

[3] J. W. Gadzuk, Solid State Commun. 15, 1011 (1974); Phys. Rev. B 10, 5030 (1974).

[4] A. Liebsch, Phys. Rev. Lett. 32, 1203 (1974).

[5] A comparison of these theories has been given by J. W. Gadzuk, Surf. Sci. (to be published).

[6] Various aspects of the surface molecule concept in chemisorption have been discussed by D. M. Newns, Phys. Rev. 178, 1123 (1969); T. B. Grimley and M. Torrini, J. Phys. C 6, 868 (1973); B. J. Thorpe, Surf. Sci. 33, 306 (1972); D. R. Penn, *ibid.* 39, 333 (1973); J. W. Gadzuk, *ibid.* 43, 44 (1974); M. J. Kelly, *ibid.* 43, 587 (1974); F. Cyrot-Lackman, M. C. Desjonqueres, and J. P. Gaspard, J. Phys. C 7, 925 (1974); T. E. Einstein, Surf. Sci. 45, 713 (1974).

[7] Surveys of chemisorption theory have been given by: T. B. Grimley, J. Vac. Sci. Technol. 8, 31 (1971); J. R. Schrieffer, *ibid.* 9, 561 (1972); N. D. Lang, Solid State Phys. 28, 225 (1973); R. Gomer, Crit. Rev. Solid State Sci. 4, 247 (1974); J. W. Gadzuk, in *Surface Physics of Materials*, edited by J. M. Blakely (Academic, New York, 1975); J. R. Schrieffer and P. Soven, Phys. Today 28, 24 (1975); J. R. Smith, in *Topics in Applied Physics*, edited by R. Gomer (Springer, Berlin, 1975).

[8] B. J. Waclawski, T. V. Vorburger, and R. J. Stein, J. Vac. Sci. Technol. 12, 301 (1975); W. F. Egelhoff and D. L. Perry, Phys. Rev. Lett. 34, 93 (1975).

[9] M. M. Traum, N. V. Smith, and F. I. DiSalvo, Phys. Rev. Lett. 32, 1241 (1974).

[10] J. E. Rowe, M. M. Traum, and N. V. Smith, Phys. Rev. Lett. 33, 1333 (1974).

[11] U. Fano and J. W. Cooper, Rev. Mod. Phys. 40, 441 (1968).

[12] It is to be noted that by simple commutation relations $\vec{P}_{op} = m\dot{\vec{x}} = (m/i\hbar)[\vec{x}, H] = -(m\omega/i)\vec{x}$. Also $[\vec{P}_{op}, H] = -\hbar\omega\vec{P}_{op} = (\hbar/i)\vec{\nabla}V$. Thus, aside from multiplicative constants, matrix elements of $\hat{\epsilon}\cdot\vec{x}$, $\hat{\epsilon}\cdot\vec{P}_{op}$, and $\hat{\epsilon}\cdot\vec{\nabla}V$ are formally equivalent. The only reason one operator is chosen over the other is the purely technical one, which depends on the approximate wave functions used in the matrix elements.

[13] For instance the e_g group consists of $d_{x^2-y^2} = 1/\sqrt{2}\,[Y_{22} + Y_{2-2}]$ with $n(m' = \pm 2) = 1/\sqrt{2}$ and $d_{z^2} = Y_{20}$ with $n(m' = 0) = 1$. The t_{2g} group consists of $d_{xz} = -1/\sqrt{2}\,(Y_{21} - Y_{2-1})$, $d_{xy} = 1/i\sqrt{2}\,(Y_{22} - Y_{2-2})$, and $d_{yz} = -1/i\sqrt{2}\,(Y_{21} + Y_{2-1})$.

[14] E. U. Condon and G. H. Shortley, *The Theory of Atomic Spectra* (Cambridge U. P., Cambridge, 1967), p. 178.

[15] H. A. Bethe and R. Jackiw, *Intermediate Quantum Mechanics* (Benjamin, New York, 1968), p. 66.

[16] P. V. S. Rao and J. T. Waber, Sur. Sci. 28, 299 (1971).

[17] B. J. Waclawski and J. F. Herbst, Phys. Rev. Lett. (to be published).

[18] P. H. Citrin and D. R. Hamann, Phys. Rev. B 10, 4948 (1974).

[19] In Ref. 5, the initial versus final state dominance has been discussed. In the text of the present paper, the Ag on LiF system has been suggested as a good candidate for partial-wave interferences. The $3d$ and $4d$ shells of Xe adsorbed on or implanted in a host are also possibilities. If there is a strong crystal field present, then the lattice effects in the final state discussed by Liebsch (Ref. 4) might be expected. To differentiate between final-state lattice effects and partial wave interferences, the ARPS should be taken at several photon energies (above the f threshold). In the theory of Liebsch, the ARPS should change shape with $h\nu$ whereas in the present theory, the absolute intensity but not the shape changes with $h\nu$, provided the f channel remains dominant.